# Simultaneous Registration and Segmentation by L1 Minimization

Pratik Shah, Mithun Das Gupta

John F. Welch Technology Center, GE Global Research, Bangalore, India
{pratik.shah, mithun.dasgupta}@ge.com

**Abstract.** This paper studies the problem of simultaneously registering and segmenting a pair of images despite the presence of non-smooth boundaries. We assume one of the images is well segmented by automated algorithm or user interaction. This image acts as an atlas for the segmentation process. For the remaining images in the set, we propose a novel L1 minimization based technique, which leverages the fact that the other image is not closely segmented but has a reasonably 'thin' boundary around it. The images are allowed to have non-rigid transformations amongst each other. We extend the two image formulation to multiple image registration and segmentation by introducing a low rank prior on the error matrix. We compare against rigid as well as non-rigid registration techniques. We present results on multi-modal real medical data.

## 1 Introduction

Simultaneous registration and segmentation of anatomical structures has garnered a lot of interest in the medical image community [1,2]. The concurrent application of registration and segmentation stems from the fact that though the underlying anatomical structure remains same, the acquired images can be very different owing to the variations in scanners, patient movements, etc. Most of these methods deal with rigid deformations taking forward the seminal work presented by Yezzi et al. [1]. [3] propose a Bayesian formulation for simultaneous inhomogeneity correction, registration, and segmentation. The registration was confined to be affine only. Recently much focus has been shifted to non-rigid deformations. [2] propose a PDE based method with the key contribution of an image matching term agnostic to absolute intensity. [4] propose a unified variational approach for image smoothing, segmentation and registration, wherein they impose pairwise registration and contour matching smoothing constraints. We propose a joint registration-segmentation formulation, where the only additional term to the registration cost is a penalty on the `area' of the region which is to be segmented `out'. By segmenting out we mean the part which does not match the region inside the atlas. In essence, if we constrain the over-segmentation present in the target image to be `thin', we can employ a sparsity prior in our cost function.

adfa, p. 1, 2011.

## 2 Sparsity Prior for Boundary

Consider the generic registration problem. Assume two images $I_1(x)$ and $I_2(x)$ of the same spatial resolution such that $\{x:\{a,b\} \in [N,M]\}$. Let the displacement field $u(x)$ be defined such that the following cost is minimized

$$C_{reg}(u) = \frac{1}{2} \int_{x\in[N,M]} \underbrace{(I_1(x) - I_2(x))^2 dx}_{data\ term} + \alpha \underbrace{Tr(\nabla u \nabla u^T)\, dx}_{continuity} \quad (1)$$

Let the two images to be registered lie in different spatial resolutions. This situation can be handled by padding the smaller spatial resolution image by appropriate zeros such the resolutions are matched again. This can potentially lead to non-optimal cost function since the images might have many dark regions which now seem to match because of the zero padding. Another solution is to put a mask around the larger image such that only region inside the mask is used for the registration process. Let us assume that this mask is known, $I_1$ is the larger fixed image, $I_2$ is the smaller moving image and the matching should be done only within this mask. The modified data term can be written as

$$C_{data}(u) = \frac{1}{2} \int_{x\in\text{mask}} \underbrace{(I_1(x) - I_2(x-u))^2 dx}_{data\ term} + \frac{1}{2} \int_{x\notin\text{mask}} I_1(x)^2 dx \quad (2)$$

Note the second term in Eq. 2 is independent of the displacement field u. Consequently, if the mask is known, the optimization inside the mask remains exactly same as the generic registration problem. Though for an unknown mask the optimization still remains ill-posed. This problem becomes more pronounced if the region near the boundary is deforming as well and is of similar intensity (Fig. 1). Alternatively, we can solve Eq. 2 treating mask $(m)$ as an unknown. We impose sparsity constraint on

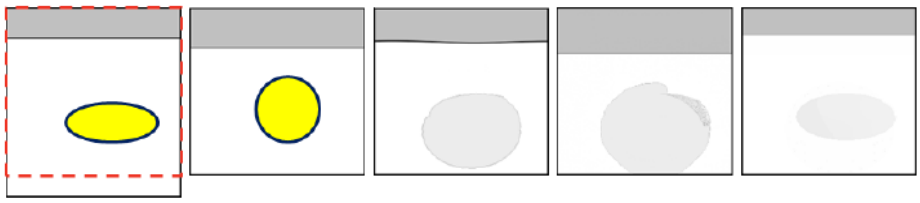

**Fig. 1.** From left to right: the first image $I_1$ is larger than the second image $I_2$. The red dotted box indicates the unknown mask within which the problem is simple registration. Note the yellow object and the gray bar put opposing forces on the registration cost term. Registration results: (third-fifth) Demons algorithm, 2-sided Demons and proposed method.

area of the region outside the mask $m$ by incorporating the $L_1$ norm constraint. For ease of exposition we define a new term $\bar{m} \stackrel{\text{def}}{=} \{I_1(x) | x \notin m\}$.

$$C_{reg}(u,\bar{m}) = \frac{1}{2}\int_{x\notin\bar{m}} (I_1(x) - I_2(x-u))^2 dx + \alpha Tr(\nabla u \nabla u^T) dx + \lambda|\bar{m}|_1 \quad (3)$$

Here $\alpha$ is the weight for the smoothness of the displacement field $u$ and $\lambda$ is the weighting for the sparsity of the area outside the mask. Further assume that we generate the image corresponding to the region outside the mask and call it the error image $e$. Given such a transformation the new cost function can be concisely written as

$$C_{reg}(u,\mathrm{e}) = \frac{1}{2}\|(I_1 - \mathrm{e}) - I_2(u)\|^2 + \lambda|e|_1 + \alpha\frac{1}{2}\|\nabla u\|^2 \quad (4)$$

We propose to solve this problem by the half quadratic method [5] which separates the discontinuous norm term from the continuous data term. Let us introduce an auxiliary variable $w$ in the registration term, such that $w = e$. The new optimization problem which we want to solve can be written as

$$C_{reg}(u,\mathrm{e},\mathrm{w}) = \frac{1}{2}\|(I_1 - \mathrm{w}) - I_2(u)\|^2 + \alpha\frac{1}{2}\|\nabla u\|^2 + \xi\frac{1}{2}\|\mathrm{w} - \mathrm{e}\|^2 + \lambda|e|_1 \quad (5)$$

Eq. 5 can now be split into two sub-problems

$$C_{reg}(u,\mathrm{w}) = \frac{1}{2}\|(I_1 - \mathrm{w}) - I_2(u)\|^2 + \alpha\frac{1}{2}\|\nabla u\|^2 + \xi\frac{1}{2}\|\mathrm{w} - \mathrm{e}\|^2 \quad (6)$$

$$C_{reg}(\mathrm{e}) = \lambda|e|_1 + \xi\frac{1}{2}\|\mathrm{w} - \mathrm{e}\|^2 \quad (7)$$

### 2.1 $C_{reg}(u,w)$ sub-problem

Minimization w.r.t. $u$: The problem with respect to $u$ is a standard registration problem. We implemented the `Demon's' registration algorithm for the non-rigid deformation estimation at each step. In registration literature, the image which moves owing to the estimated deformation is called the moving image $M$ ($I_2$ in our case) and the image which is held fixed to which the moving image is compared to is called the fixed image $F$ ($(I_1 - w)$ in our case). For a given point $p$ in fixed image $F$, let $s$ be the intensity and corresponding intensity $r$ in moving image $M$. The velocity (optical flow) required to match the corresponding point in $M$ is derived by Thirion [6]. We used improved demons algorithm proposed by Cachier [7], where the local velocity $v_p$ at the location $p$ is denoted as

$$v_p = \frac{(r-s)\nabla s}{|\nabla s|^2 + \beta^2|r-s|^2} + \frac{(r-s)\nabla \mathrm{r}}{|\nabla \mathrm{r}|^2 + \beta^2|r-s|^2} \quad (8)$$

Here, $\nabla$ is gradient operator and $\beta$ is normalization factor to balance two forces, an internal edge based force and image difference based force. The registration is achieved iteratively by minimizing local velocity at all pixels.

Minimization w.r.t. $w$: To estimate $w$, we utilize the fact that Eq. 6 is strictly convex with respect to $w$ for fixed $u$, and hence a unique minimizer at each step can be computed.

$$\frac{\partial C_{reg}(u,w)}{\partial w} = 0 \Rightarrow w = \frac{\xi e + (I_1 - I_2(u))}{1+\xi} \quad (9)$$

### 2.2 $C_{reg}(e)$ sub-problem

The $C_{reg}(e)$ subproblem in Eq. 7 is an $L_1$norm minimization problem. A similar problem, known as the penalty formulation, was elegantly solved in linear time by the algorithm proposed by Duchi et al. [8]. The penalty formulation is stated as, for a fixed vector $v$, $\min_x \frac{1}{2}\|v-x\|^2, s.t. |x|_1 \leq z$. Ignoring the trivial case where $|v|_1 \leq z$ for which the solution is $x = v$, there exists for each $z$ a particular $\theta$ such that $\min_x \frac{1}{2}\|v-x\|^2 + \theta|x|_1$ has the same solution. The solution of this penalized formulation is directly obtained by applying the (component-wise) soft-thresholding operator [9]

$$S_\theta(v) = \text{sign}(v).\max\{0, |v| - \theta\} \quad (10)$$

The signum function $sign(c) \stackrel{\text{def}}{=} c/\!/\!/c/\!/\!/$ is also defined component-wise, and by convention the elements of $sign(0)$ can be chosen arbitrarily between -1 and 1. The equivalence leads to finding $\theta$ such that $|S_\theta(v)|_1 = z$.

## 3 Group Segmentation

Our method can be modified to tackle a group segmentation and registration problem. Collecting the $k$ images into a matrix $Y = [I_1, I_1 \dots I_k]$, the deformations into $U = [u_1, u_1 \dots u_k]$, the transformed atlas for matching to individual fixed image into $X = [I_a(u_1), I_a(u_2) \dots I_a(u_k)]$ and the error vectors into a matrix $E = [e_1, e_1 \dots e_k]$, we write the group problem, for $k$ images and one atlas as $C_{grp}(U,E) = \frac{1}{2}\|(Y-E) - X\|^2 + \alpha\frac{1}{2}\|\nabla U \nabla U^T\|^2$. Without any further constraints, the group formulation is just a combination of $k$ individual problems. For a medical application, where the images are captured with close temporal and spatial proximity, the images can be considered correlated to each other, under non-rigid transformations. We assume that the error vector obtained from one segmentation is similar to the error vectors obtained from the other images. In other words, $e_i \sim e_j, \forall i,j, \in [1,k]$. This leads to the additional group constraint $rank(E) < \rho$. Integrating the rank constraint into the framework the new cost function for the group registration becomes

$$C_{reg}(U,E) = \frac{1}{2}\|(\mathrm{Y}-\mathrm{E}) - \mathrm{X}\|^2 + \alpha\frac{1}{2}\|\nabla \mathrm{U} \nabla \mathrm{U}^T\| + \mu\mathrm{rank}(E) + \lambda\|E\|_1 \quad (11)$$

Applying a variable separation technique, similar to the single image case, the modified optimization can be written as two separate sub-problems

$$C(U,W) = \mu\text{rank}(W) + \frac{1}{2}\|(\mathrm{Y}-\mathrm{W})-\mathrm{X}\|^2 + \alpha\frac{1}{2}\|\nabla\mathrm{U}\nabla\mathrm{U}^T\| + \xi\|\mathrm{W}-\mathrm{E}\|^2 \quad (12)$$

$$C(E) = \xi\|\mathrm{W}-\mathrm{E}\|^2 + \lambda\|E\|_1 (13)$$

$C(E)$ : The minimization with respect to each error vector $e_i$ is performed similar to the case for one image.
$C(U,W)$, wrt $U$ : This sub-problem is the registration step and is also performed per image.
$C(U,W)$, wrt $W$: The minimization with respect to $W$ is the most important part of the group joint registration and segmentation framework. Convex relaxation for the rank constraint was proposed by Peng at al. [10]. The rank constraint can be replaced by the nuclear norm which is the sum of the singular values $\|W\|_* \stackrel{\text{def}}{=} \sum_{i=1}^{m}\sigma_i(W)$. The modified cost function can be written as

$$C(W) = \mu\|W\|_* + \xi\|\mathrm{W}-\mathrm{E}\|^2 + \frac{1}{2}\|(\mathrm{Y}-\mathrm{W})-\mathrm{X}\|^2 \quad (14)$$

We adopt an accelerated proximal gradient (APL) [11] based method to solve Eq. 14. The APL technique replaces the quadratic equality constraint by a convex upper bound of it. Let us simplify the notation and contain all the constraints into one function $f(W) = \xi\|\mathrm{W}-\mathrm{E}\|^2 + \frac{1}{2}\|(\mathrm{Y}-\mathrm{W})-\mathrm{X}\|^2$. The simplified cost function can be written as $C(W) = \mu\|W\|_* + \mathrm{f(W)}$. The equality constraint set $f(W)$ is convex and smooth with Lipschitz continuous gradient and hence $\|\nabla f(W_1) - \nabla f(W_2)\| \leq C_L\|W_1 - W_2\|$ , where $C_L$ is the Lipschitz constant. Instead of directly ing $C(W)$, APL minimizes a sequence of separable quadratic approximations to it, denoted as $Q(W,Z)$, formed at specially chosen points $Z$:

$$Q(W,Z) = f(Z) + \langle\nabla f(Z), W-Z\rangle + \frac{C_L}{2}\|W-Z\|^2 + \mu\|W\|_* \quad (15)$$

It can be shown that for any Z, Q(W, Z) upper bounds C(W). If we define $\mathrm{G} = \mathrm{Z} - \frac{1}{\mathrm{C_L}}\nabla\mathrm{f(Z)}$, then

$$\underset{W}{arg\,min}\, Q(W,Z) = \underset{W}{arg\,min}\{\mu\|W\|_* + \frac{C_L}{2}\|W-G\|^2\} \quad (16)$$

The solution for the particular problem can be found by iteratively evaluating the matrix $G$ and then projecting its eigen vectors to a low ranked space spanned by the top few eigen values which are larger in magnitude than $\mu/C_L$. For our particular problem, $C_L = 4(\xi+\lambda)$. For accelerating the general proximal gradient technique, Lin et al. [11] propose an acceleration step. This modification is achieved by starting with a large value of $\mu = \mu_0$, the weighting parameter for the norm constraint and then gradually decreasing it to some predefined floor value $\bar{\mu}$. The convergence for the APG method can be invoked for the following theorem:

***Theorem 1***. *Let* $F(W) = min\ \bar{\mu}\|W\|_* + \xi\|W-E\|^2 + \frac{1}{2}\|(Y-W)-X\|^2$
*Then,* $\forall k > k_0 \stackrel{\text{def}}{=} \frac{log(\mu_0/\bar{\mu})}{log\frac{1}{\eta}}$

$$F(W_k) - F(W^*) \leq \frac{2C_L \left\| W_{k_0} - W^* \right\|^2}{(k - k_0 + 1)^2} \qquad (17)$$

*Where, $W^*$ is any solution to Eq. 12, $\mu_{k+1} = \eta\mu_k$ and $C_L = 4(\xi + \lambda)$.*

Thus for any $\epsilon > 0$, when $\forall k > k_0 + \sqrt{\frac{2C_L \left\| W_{k_0} - W^* \right\|^2}{\epsilon}}$, we can guarantee that $F(W_k) < F(W^*) + \epsilon$.

## 4 Experiments and Results

For the first set of experiments, we choose two kinds of images with very different characteristics, namely: magnetic resonance (MR) images, and Lena (Fig. 2). The Lena image is deformed to generate the fixed images. The MR image is obtained from the patient scan at a different time. We quantified our

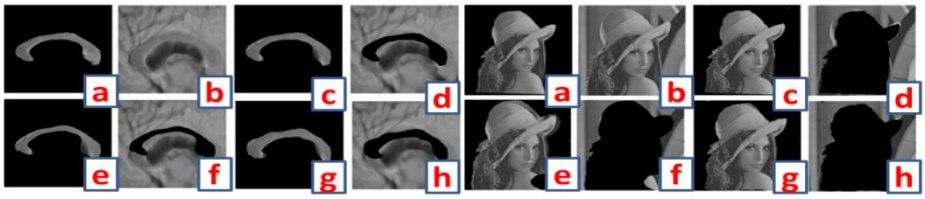


| Image | rigid | nonrigid | proposed |
|---|---|---|---|
| MR | 0.47389 | 0.7064 | 0.81566 |
| lena | 0.93672 | 0.93151 | 0.95857 |

**Fig. 2.** Comparison of different algorithms for segmentation and registration on 2D examples. For each image class (a) segmented atlas, (b) to be segmented image with boundary, (c,d) rigid registration: segmented and registered object, extracted background respectively, (e,f) non-rigid registration: segmented and registered object, extracted background respectively, (g,h) proposed method: segmented and registered object, extracted background respectively. Bottom Row: comparison with registration.

algorithm performance and compared it against rigid and non-rigid registration algorithms (without the novel sparsity prior) using dice coefficient. We used area of the interested object as a metric for dice coefficient. The quantification results suggest that our approach performs consistently better than simple registration.

Circle of Willis: Carotid and vertebra-basilar arteries are the main trunk arterial lines to supply blood to brain. They form circle at the base of the brain also known as circle of Willis (COW). If any vessel is blocked or occluded or partially blocked, the circular formation of vessels makes possible to circulate blood to all higher level arteries (collateral circulation) and thus enables proper brain functioning1. Intra-arterial digi-

[1] http://www.strokecenter.org/professionals/brain-anatomy/blood-vessels-of-thebrain/

tal subtraction angiography (IADSA) is the gold standard to access the vascular pathology in intracranial region [12]. However, it provides projection based information.

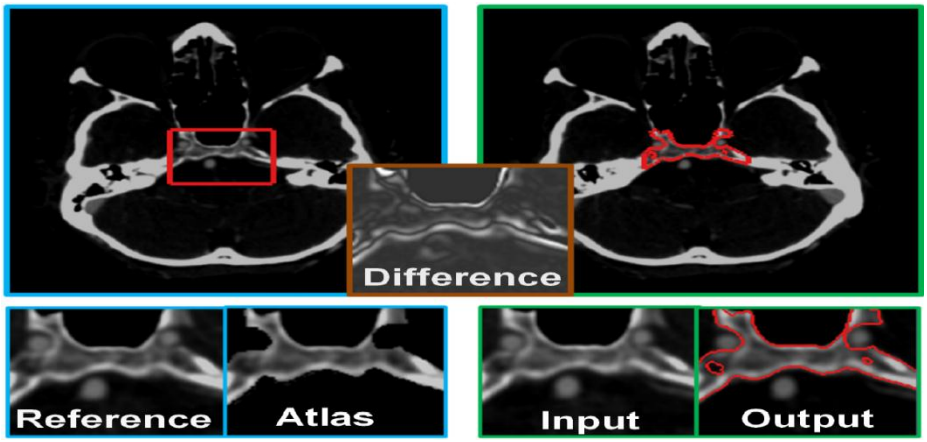


**Fig. 3.** Sphenoid Bone removal 2 image experiment. The blue outline images were used to create the atlas by manual segmentation. The green outline images form the output images. The red rectangle in the left most image shows the ROI which is the reference image (bottom left). The manual segmentation of the reference image generates the Atlas. The input image to the system is the ROI from the new image. The output of our method is shown in bottom right. The inset image with the brown outline shows the difference of the reference and the input image (with window leveling to show the absolute difference).

CT angiography is currently widely used to visualize the vessels in 3D. Region of interest based 3D visualization either by volume rendering or Maximum intensity projection (MIP) of COW hinders by surrounded soft bone, especially sphenoid bone. Fig. 3 shows single frame result for Sphenoid bone suppression. Given the Volume of interest (VOI) for sphenoid bone and 2D atlas, our approach performs non rigid transformation on atlas to match the bone in the incoming input images. Though intracranial carotid artery is very close to bone in spatial and intensity domain, the prior of sparse deformation forced it to be out from the bone definition. The multi-image results with the MIP projection are shown in Fig. 4.

## 5 Conclusion and Future Work

In this work, we present a combined registration and segmentation framework, which can be used in multiple application domains. The proposed model stands out for its simplicity as well as performance. The applicability of the method is further enhanced by the fact that it has a modular structure, which enables any registration algorithm to be fed into it. We further introduce a group segmentation-registration algorithm, which introduces a unique way of combining low norm and low rank constraints. We keep the actual evaluation of the interplay of different registration algorithms with our method as a future work.

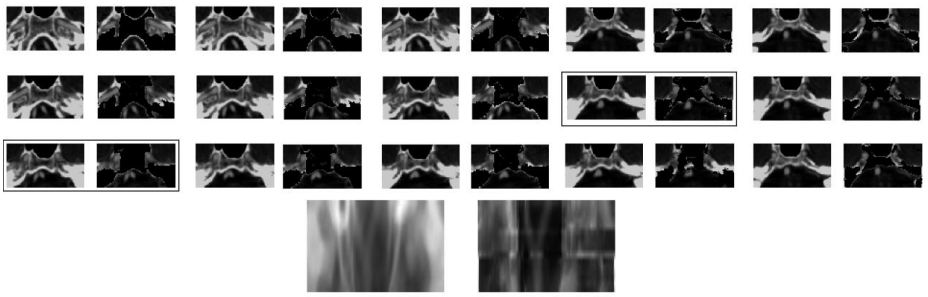

**Fig. 4.** Sphenoid Bone removal. Each pair of image shows the original frame and the bone removed frame. The two pairs in boxes are manually generated. The last two images show the MIP projection before and after bone removal.

## References


1. Yezzi, A., Zollei, L., Kapur, T.: A variational framework for joint segmentation and registration. In: IEEE Mathematical Methods In Biomedical Image Analysis.(2001) 44-51
2. 2. Wang, F., Vemuri, B.C.: Simultaneous registration and segmentation of anatomical structures from brain MRI. In: MICCAI. (2005) 17-25
3. Pohl, K., Fisher III, J., Levitt, J., Shenton, M., Kikinis, R., Grimson, W., Wells III, W.: A unifying approach to registration, segmentation, and intensity correction. MICCAI (2005) 310-318
4. Lord, N.A., Ho, J., Vemuri, B.C.: USSR: A uni_ed framework for simultaneous smoothing, segmentation, and registration of multiple images. ICCV (2007) 1-6
5. Krishnan, D., Fergus, R.: Fast image deconvolution using Hyper-Laplacian priors. Advances in Neural Information Processing Systems (2009) 1033-1041
6. Thirion, J.P.: Image matching as a di_usion process: an analogy with Maxwell's demons. Medical Image Analysis (1998) 243-260
7. Cachier, P., Pennec, X., Ayache, N.: Fast Non Rigid Matching by Gradient Descent: Study and Improvements of the "Demons" Algorithm. Technical Report RR-3706, INRIA (1999)
8. Duchi, J., Shwartz, S.S., Singer, Y., Chandra, T.: E_cient projections onto the L1-ball for learning in high dimensions. In: ICML '08. (2008) 272-279
9. Chambolle, A., DeVore, R.A., Lee, N.Y., Lucier, B.J.: Nonlinear wavelet image processing: Variational problems, compression, and noise removal through wavelet shrinkage. IEEE Trans. Image Processing 7 (1996) 319-335
10. Peng, Y., Ganesh, A.,Wright, J., Xu, W., Ma, Y.: Rasl: Robust alignment by sparse and low-rank decomposition for linearly correlated images. In: CVPR. (2010)
11. Lin, Z., Ganesh, A.,Wright, J.,Wu, L., Chen, M., Ma, Y.: Fast convex optimization algorithms for exact recovery of a corrupted low-rank matrix. preprint (2009)
12. Ghazali, R.M., Shuaib, I.L.: comparison between 3d tof magnetic resonance angiography and intraarterial digital subtraction angiography in imaging the circle of willis. Malaysian Journal of Medical Sciences 10 (2003) 37-42